Optimization of Cascade Integer Resolution with Three Civil GPS Frequencies

Jaewoo Jung, Per Enge, Stanford University
Boris Pervan, Illinois Institute of Technology

BIOGRAPHY

Dr. Jaewoo Jung received his B.S. in Aerospace Engineering in Boston University, and his M.S. and Ph.D. in Aeronautics and Astronautics Engineering from Stanford Universiy. He is now working at Trimble Navigation, Ltd. Dr. Per Enge is an Associate Professor in the Department of Aeronautics and Astronautics Engineering at Stanford University. He received his B.S. in electrical engineering from the University of Massachusetts at Amherst, and his M.S. and Ph.D., both in Electrical Engineering, from the University of Illinois at Urbana-Champaign. Dr. Boris Pervan is an Assistant Professor of Mechanical and Aerospace Engineering at the Illinois Institute of Technology in Chicago. He received B.S. from the University of Notre Dame, M.S. from the California Institute of Technology, and Ph.D. in Aeronautics and Astronautics Engineering from Stanford University.

ABSTRACT

In the near future, there will be two more civil GPS signals in addition to the current one at the L1 frequency (1575.42 MHz). The second civil signal will be broadcast at the L2 frequency (1227.60 MHz), and the third civil signal will be broadcast at the recently-selected Lc frequency (1176.45 MHz). With three civil frequencies, a user can generate three beat frequency signals. The L1 and L2 carrier frequencies are processed to create the Widelane (WL) with wavelength of 86 centimeters. The combination of the L1 and Lc carrier frequencies yields the second beat frequency with 75 centimeters in wavelength (Medium Lane, ML). The combination of the L2 and Lc carrier frequencies yields the third beat frequency with 5.9 meters in wavelength (Extra Widelane, EWL).

In earlier research [8], an instantaneous geometry-free carrier-phase DGPS integer ambiguity resolution technique was developed utilizing the multiple available beat frequencies. This technique, known as Cascade Integer Resolution (CIR), resolves the integer ambiguities successively from the longest to the shortest beat wavelength. The performance of CIR was examined in the earlier study, and it was shown that CIR can be used to resolved the Lc integer ambiguity with probability of wrong integer resolution of 1E-4 up to 2.4 kilometers from a reference station. It can also resolve the WL integer ambiguity up to 22 kilometers, and the EWL integer ambiguity beyond that, with the same probability of incorrect integer resolution.

Performance degradation of the CIR over distance mainly comes from the spatial decorrelation of ionospheric error (residual differential troposphere error is eliminated by the geometry-free CIR process). This paper focuses on recent improvements to CIR performance to extend service volume and reduce the probability of incorrect integer resolution. First, effect of decrease in measurement error on performance of the CIR is examined. Then, the spatial gradient of the residual differential ionosphere error, which was assumed to have a fixed standard deviation of 2 parts per million in the earlier research, is estimated by using measurements from two different user locations. Estimation of ionospheric spatial decorrelation is integrated into the CIR process. With these enhancements, performance of the CIR increased. With the probability of incorrect integer ambiguity resolution of 1E-4, the optimized CIR can resolve the Lc integer up to 4 km (increases of 2.4 km) and the WL integer up to 40 km (increase of 22 km).

DEFINITION OF THE CIR

In earlier research, Cascade Integer Resolution (CIR) was developed. The CIR is a geometry-free, instantaneous integer ambiguity resolution method. It utilizes beat frequencies of the three civil GPS signals (Table 1) to resolve the integer ambiguity

A real-valued solution for the extra widelane integer, N_{EWL}, is estimated by subtracting the Lc code pseudorange measurement from the EWL measurement. The Lc code is used in the CIR as the principle pseudorange measurement, as it will have improved multipath performance due to its higher clock rate of 10.23 MHz. Assuming the double differenced measurements are used, the EWL integer estimation is described in the following equations.

$$\lambda_{EWL}\phi_{EWL} = R + \lambda_{EWL}N_{EWL} - \Upsilon_{EWL}I_{L1} + T + \nu_{EWL}$$

$$\rho_{Lc} = R + \Upsilon_{1c}I_{L1} + T + \mu_{Lc}$$

$$\phi_{EWL} - \frac{\rho_{Lc}}{\lambda_{EWL}} = \hat{N}_{EWL} \quad (1)$$

$$\hat{N}_{EWL} = N_{EWL} - \frac{(\Upsilon_{EWL} - \Upsilon_{1c})}{\lambda_{EWL}}I_{L1} + \frac{(\nu_{EWL} - \mu_{Lc})}{\lambda_{EWL}} \quad (2)$$

- λ is wavelength in meter
- ϕ is carrier phase measurement
- R is geometric range
- Υ is a scale factor for ionospheric error
- I_{L1} is ionospheric error at the L1 frequency
- T is tropospheric error
- ν is carrier phase multipath and receiver error
- ρ is pseudorange in meter
- μ is code multipath and receiver error

If the combined error from both the Lc code and the EWL measurements is smaller than one-half of an EWL wavelength (5.86 m), the goal is to obtain the correct EWL integer by rounding the real-valued solution. Note that the residual differential tropospheric term, which is independent of frequency, is eliminated when the Lc code and the EWL measurements are differenced.

With a correct integer, the EWL measurement is used as the pseudorange measurement, and is subtracted from the WL measurement to get a real-valued solution for the WL integer ambiguity.

$$\lambda_{WL}\phi_{WL} = R + \lambda_{WL}N_{WL} - \Upsilon_{WL}I_{L1} + T + \nu_{WL}$$

$$\phi_{WL} - \frac{\lambda_{EWL}}{\lambda_{WL}}(\phi_{EWL} - N_{EWL}) = \hat{N}_{WL} \quad (3)$$

$$\hat{N}_{WL} = N_{WL} - \frac{(\Upsilon_{WL} - \Upsilon_{EWL})}{\lambda_{WL}}I_{L1} + \frac{(\nu_{WL} - \nu_{EWL})}{\lambda_{WL}} \quad (4)$$

Again, if the combined error from the EWL and WL measurements is smaller than one-half of a WL wavelength (86 cm), a correct WL integer is obtained by rounding the real-valued solution.

With a correct integer, the WL measurement is used as the pseudorange measurement to resolve the L1, L2 or Lc integer ambiguity. The Lc case is shown as an example.

$$\phi_{Lc} - \frac{\lambda_{ML}}{\lambda_{Lc}}(\phi_{ML} - N_{ML}) = \hat{N}_{Lc} \quad (5)$$

$$\hat{N}_{Lc} = N_{Lc} - \frac{(\Upsilon_{Lc} - \Upsilon_{ML})}{\lambda_{Lc}}I_{L1} + \frac{(\nu_{Lc} - \nu_{ML})}{\lambda_{Lc}} \quad (6)$$

Since this method resolves the integer ambiguities from the longest to the shortest wavelength successively using the previous measurement, it is defined as the Cascade Integer Resolution (CIR).

Table 1. Three Beat Frequencies

Beat Frequency	Frequency (MHz)	Wavelength (m)
Extra Widelane (EWL) L2-Lc	51.15	5.86
Widelane (WL) L1-L2	347.82	.862
Mediumlane (ML) L1-Lc	348.97	.751

INTEGRITY OF THE CIR PROCESS

Analysis Setup

The CIR with three civil GPS signals uses one-on-one combination of three carrier frequencies to form three beat frequencies. However, the generated beat frequencies are not linearly independent. For example, in the first and second rows of Table 2, the EWL and WL frequencies can be added together to produce the ML frequency. The effect of linearly dependent beat frequency measurements in the CIR process is examined by a covariance analysis of measurement error. The state vector, **u**, observation matrix, H, and measurement vector, **z** used in the analysis are

Table 2. Three Beat Frequencies

	f_{L1}	f_{L2}	f_{Lc}
EWL	0	1	-1
WL	1	-1	0
ML	1	0	-1

described in Equations (7) and (8). The analysis is also used to calculate the probability of incorrect integer resolution of each CIR step, verifying integrity of the CIR in an ensemble sense, in contrast to the conditional probability analysis developed in the earlier research, whish was a Bayesian result.

$$z = Hu + \delta z \tag{7}$$

$$\begin{bmatrix} \rho_1 \\ \rho_2 \\ \rho_c \\ \phi_1 \\ \phi_2 \\ \phi_c \\ \hat{I}_1 \end{bmatrix} = \begin{bmatrix} 1 & 1 & 0\ 0\ 0 \\ 1 & \Upsilon_{12} & 0\ 0\ 0 \\ 1 & \Upsilon_{1c} & 0\ 0\ 0 \\ 1/\lambda_1 & -1/\lambda_1 & 1\ 0\ 0 \\ 1/\lambda_2 & -\Upsilon_{12}/\lambda_2 & 0\ 1\ 0 \\ 1/\lambda_c & -\Upsilon_{1c}/\lambda_c & 0\ 0\ 1 \\ 0 & 1 & 0\ 0\ 0 \end{bmatrix} \begin{bmatrix} R \\ I_1 \\ N_1 \\ N_2 \\ N_c \end{bmatrix} + \begin{bmatrix} \delta\rho_1 \\ \delta\rho_2 \\ \delta\rho_c \\ \delta\phi_1 \\ \delta\phi_2 \\ \delta\phi_c \\ \hat{\delta I}_1 \end{bmatrix} \tag{8}$$

- **z** is a measurement vector, including six double difference measurements, three code and three carrier phase. An *a priori* knowledge of linear gradient of standard deviation of residual differential ionospheric delay is also included.
- H is an observation matrix. Scale factors for ionospheric effect on frequencies other than the L1 are included.
- **u** is a state vector, containing pseudorange, R, residual differential ionospheric effect at the L1 frequency, I_1, and three integer ambiguities for the L1, L2 and Lc carrier phase measurements, N_1, N_2, and N_c.
- δz is a measurement error vector.

A covariance matrix of the state estimation error, P_u, is calculated from a covariance matrix of the measurement error, P_z. Calculation of the P_z and the P_u matrices are shown in Equations (9) and (10). The six double difference measurements, three code and three carrier phase, are assumed to be independent, and measurement error models developed in the earlier research are used to form the measurement error vector, δz. The double difference carrier phase multipath and receiver error is assumed to be bounded by a Gaussian distribution with standard deviation of 2% of wavelength. The linear gradient of standard deviation of residual differential ionospheric error is 2 ppm, and therefore the standard deviation of the residual differential ionosphere error is calculated by multiplying its gradient with the baseline distance.

$$P_z = E[\delta z \delta z] \tag{9}$$

$$P_u = (H^T (P_z)^{-1} H)^{-1} \tag{10}$$

$$P_i = \begin{bmatrix} E[\delta N_1 \delta N_1] & E[\delta N_1 \delta N_2] & E[\delta N_1 \delta N_c] \\ E[\delta N_2 \delta N_1] & E[\delta N_2 \delta N_2] & E[\delta N_2 \delta N_c] \\ E[\delta N_c \delta N_1] & E[\delta N_c \delta N_2] & E[\delta N_c \delta N_c] \end{bmatrix} \tag{11}$$

The covariance matrix of the estimation error of three double difference integers, P_i, is a subset of a covariance matrix of states, P_u. Using the P_i matrix (Equation (11)), standard deviation of the estimation error for the integer ambiguity solution for each carrier frequency maybe calculated by taking the square root of its diagonal components.

$$\sigma_{N1} = \sqrt{E[\delta N_1 \delta N_1]}$$

$$\sigma_{N2} = \sqrt{E[\delta N_2 \delta N_2]}$$

$$\sigma_{Nc} = \sqrt{E[\delta N_c \delta N_c]}$$

$$P_z = \begin{bmatrix} E[\delta\rho_1 \delta\rho_1] & 0 & 0 & 0 & 0 & 0 & 0 \\ 0 & E[\delta\rho_2 \delta\rho_2] & 0 & 0 & 0 & 0 & 0 \\ 0 & 0 & E[\delta\rho_c \delta\rho_c] & 0 & 0 & 0 & 0 \\ 0 & 0 & 0 & E[\delta\phi_1 \delta\phi_1] & 0 & 0 & 0 \\ 0 & 0 & 0 & 0 & E[\delta\phi_2 \delta\phi_2] & 0 & 0 \\ 0 & 0 & 0 & 0 & 0 & E[\delta\phi_c \delta\phi_c] & 0 \\ 0 & 0 & 0 & 0 & 0 & 0 & E[\hat{\delta I}_1 \hat{\delta I}_1] \end{bmatrix}$$

The standard deviation of the estimation error for the integer ambiguity solution for each beat frequency is also calculated by multiplying the P_i matrix with a vector containing the multiplication factor for the involved frequencies. This step forms the beat frequency. Taking the square root of this value yields the standard deviation of the estimation error. In Equation (12), this process is completed for the EWL integer ambiguity solution.

$$\sigma_{N_{EWL}} = \left(\begin{bmatrix} 0 & 1 & -1 \end{bmatrix} P_i \begin{bmatrix} 0 & 1 & -1 \end{bmatrix}^T \right)^{1/2} \tag{12}$$

$$\phi_{EWL} = 0 \times \phi_1 + 1 \times \phi_2 - 1 \times \phi_c \Rightarrow \begin{bmatrix} 0 & 1 & -1 \end{bmatrix}$$

The estimated solution of the integer ambiguity is real-valued, and it can be rounded into a correct integer if the standard deviation of the estimation error of the integer ambiguity solution is much less than 1/2. Therefore, a desired level of integrity can be specified by multiplying the standard deviation of the integer ambiguity estimation error with a factor, K_{MD}. Then, to round the real-valued solution into a correct integer with a desired level of integrity, the following relation must hold true.

$$K_{MD}\sigma_{N_{EWL}} < \frac{1}{2} \tag{13}$$

Assuming a normal distribution of estimation error, the probability of wrong integer rounding, is then the following.

$$P_{wrongN_{EWL}} = 1 - \int_{-\infty}^{K_{MD}} f(x)dx \tag{14}$$

$K_{MD} = \dfrac{1}{2\sigma_{N_{EWL}}}$ and $f(x)$ is a normal distribution function

Example: $P = 10^{-9}$ when $\dfrac{1}{2\sigma_{N_{EWL}}} \cong 6.2$ (or $K_{MD} = 6.2$)

Applying the Covariance Analysis to the CIR

The CIR uses the code measurements to resolve the EWL integer ambiguity, then uses the EWL measurement to resolve the WL integer ambiguity, and so on. Due to this cascading nature, the measurement vector, **z**, and the observation matrix, H, in the covariance analysis are updated after a successful rounding of real-valued integer ambiguity estimation to a correct integer for each beat frequency. For example, once a correct EWL integer is rounded with a desired integrity, as specified in Equation (13), probability of incorrect rounding of the estimated WL integer ambiguity solution is calculated after the following update.

$$\begin{bmatrix} z \\ N_{EWL} \end{bmatrix} = \begin{bmatrix} H \\ 0 \;\; 0 \;\; 0 \;\; 1 \;\; -1 \end{bmatrix} \begin{bmatrix} u \end{bmatrix} + \begin{bmatrix} \delta z \\ \delta N_{EWL} \end{bmatrix} \tag{15}$$

where $z' = H'u + \delta z'$

$$P_z' = E[\delta z' \delta z']$$

$$P_u' = (H'^T (P_z')^{-1} H')^{-1}$$

and P_i' is a subset of P_u'

$$\sigma_{N_{WL}} = \left(\begin{bmatrix} 1 & -1 & 0 \end{bmatrix} P'_i \begin{bmatrix} 1 & -1 & 0 \end{bmatrix}^T \right)^{1/2} \tag{16}$$

$$\phi_{WL} = 1 \times \phi_1 - 1 \times \phi_2 + 0 \times \phi_c \Rightarrow \begin{bmatrix} 1 & -1 & 0 \end{bmatrix}$$

Since N_{EWL} is rounded to a correct integer, δN_{EWL} is 0. Then probability of the wrong WL integer rounding is the following.

$$P_{wrongN_{WL}} = 1 - \int_{-\infty}^{K_{MD}} f(x)dx \tag{17}$$

The updated measurement vector, z', and observation matrix, H', is updated once again with a correct WL integer, which is rounded with a desired integrity to calculate the probability of wrong Lc integer rounding.

Integrity of the CIR Over Short Baseline Distances

Integrity of the CIR is examined by using a covariance analysis of the measurement error. The double difference measurement error model developed in the earlier research is used in the analysis. A short baseline distance between the reference and user receivers is assumed, and residual differential ionospheric effect is ignored. Probability of wrong integer rounding of each step in the CIR process is calculated. The results are shown in Table 3.

The analysis results show that resolution of the EWL integer in the CIR is highly successful, with probability of wrong integer rounding less then 10^{-15}. Resolving the WL integer has probability of wrong integer rounding equal to 6.43×10^{-5}. While the ML integer resolution has probability of wrong integer rounding of 0. This means that once the EWL and WL integer ambiguities are resolved, the ML integer is already known as it is a linear combination of the previous two terms. Therefore, the linearly dependent beat

Table 3. Integrity of the CIR Steps

Rounded Integer Ambiguity	Probability of Wrong Integer Rounding
EWL	less then 10^{-15}
WL	6.43×10^{-5}
ML	0
Lc	6.38×10^{-9}

frequency measurement, the ML measurement in this case, does not affect integrity of the CIR process, as resolution of this term is trivial and unnecessary. The Lc integer ambiguity is resolved by using the WL measurement, and probability of wrong integer rounding is 6.38×10^{-9} .

Integrity of the entire CIR process with *n* steps is then defined as follows.

$$\prod_{i=1}^{n} P_{correctInteger}(step(i)) \tag{18}$$

For example, integrity of the entire CIR process over a short distance is calculated below.

$$P_{CIR} = P_{correctN_{EWL}} \times P_{correctN_{WL}} \times P_{correctN_{ML}} \times P_{correctN_{Lc}}$$

$$P_{CIR} = (1 - 10^{-15}) \times (1 - 6.43 \times 10^{-5}) \times (1) \times (1 - 6.38 \times 10^{-9})$$

$$P_{CIR} = 0.99994 \tag{19}$$

Integrity of the CIR at a short baseline distance can be interpreted in several ways by using the results from the covariance analysis. For an accuracy requirement on the order of tens of centimeters and integrity requirement on the order of 10^{-8} , the CIR can be used to resolve the EWL integer ambiguity, since probability of wrong integer rounding is less than 10^{-15} . However, the CIR cannot be used to resolve the WL integer ambiguity for this application, since the probability of wrong integer rounding is 10^{-5} . Since the WL measurement cannot be used in this application, resolving the Lc integer ambiguity is not possible due to the aforementioned cascading nature of the CIR. For an accuracy requirement on the order of centimeters and integrity requirement on the order of 10^{-4} , the CIR can be used to resolve the EWL, WL, and Lc integer ambiguity, since integrity of the entire CIR process is 99.994% (per Equation (19)).

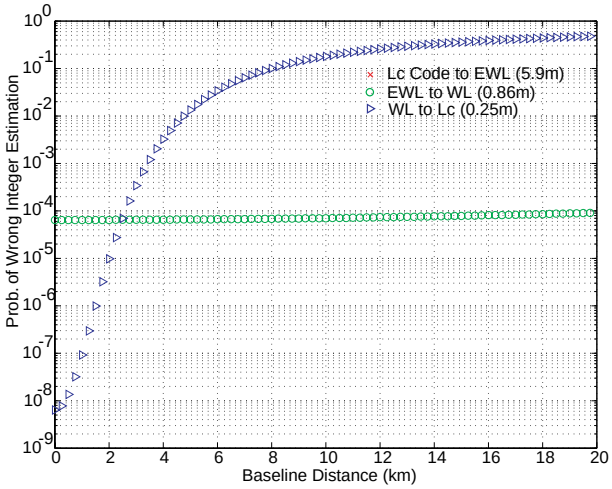

Figure 1. Integrity of the CIR Steps Over Distance

Integrity of the CIR Over Long Baseline Distance

As baseline distance between the reference and user receivers increases, residual differential ionospheric error grows. Probability of wrong integer rounding at each step of the CIR is calculated over distance, from 0 to 20 km. The results are plotted in Figure 1. Note that the probability of wrong EWL integer rounding is not shown on the plot as this value is lower than 10^{-9} even at the 20 km baseline. As expected, the probability of wrong integer rounding, or integrity risk of each step, increases over distance. As mentioned, this occurs because the standard deviation of measurement error increases over distance due to the increase in residual differential ionospheric error. Integrity of the CIR with a short baseline distance, is represented at 0 km in Figure 1.

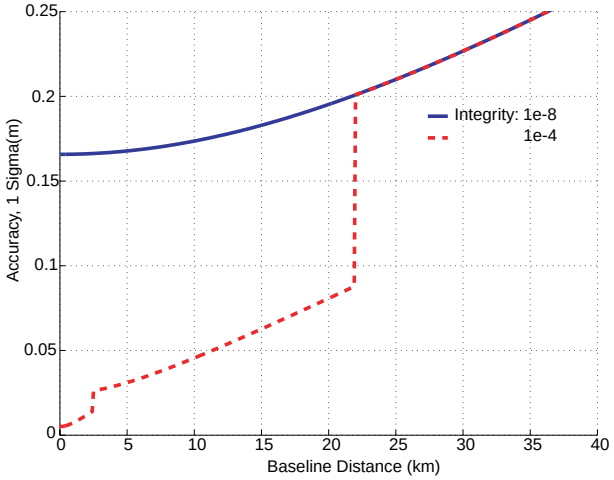

Figure 2. Level of Accuracy of the CIR Over Distance

The probability results in Figure 1 can be used to interpret integrity of the CIR over distance. For an application requiring integrity risk on the order of 10^{-8}, the EWL integer ambiguity is resolved since the probability of incorrect EWL integer resolution is less than 10^{-9} for all the tested distances. The WL integer ambiguity cannot be resolved because the probability of incorrect WL integer ambiguity is higher than 10^{-8} for all the tested distances (o in the figure). Due to the aforementioned cascading nature, the Lc integer ambiguity cannot be resolved without resolving the WL integer ambiguity.

For an application requiring integrity risk on the order of 10^{-4}, the EWL integer ambiguity is resolved since the probability of incorrect EWL integer ambiguity resolution is less than 10^{-9} for all the tested distances. The WL integer ambiguity is resolved up to 22 km, where probability of incorrect WL integer ambiguity resolution becomes higher than 10^{-4}. The Lc integer ambiguity is resolved up to 2.4 km, where probability of incorrect Lc integer ambiguity resolution becomes higher than 10^{-4}. Figure 2 summarizes the above results.

EFFECT OF MULTIPATH AND RECEIVER ERROR REDUCTION ON INTEGRITY OF THE CIR

The white noise portion of the double difference measurement error is reduced by using time averaging. Figure 3 shows the effect of time averaging on the double difference of the L1 carrier phase measurement. The upper figures represent double difference carrier phase measurements without time averaging, in time and frequency domain (power spectral density), from left to right, respectively. The lower figures represents the same measurements with the time averaging applied. A time constant of 200 seconds is used. The time averaged double difference carrier phase measurements show decrease in measurement error in the time domain, and decrease in power of high frequency components. These results indicate that the white noise portion of measurement error, such as receiver error due to thermal noise and fast varying component of multipath, is reduced. However, they also indicate biased noise, such as the slow varying component of multipath is not reduced.

For a short baseline distance, carrier phase multipath is the limiting error source for performance of CDGPS. Multipath mitigation is an ongoing research topic. For example, research by Axelrad [1] uses the signal to noise ratio to eliminate the slow varying component of multipath. Work by Ray [10] uses multiple antennae to reduce multipath effect for a static receiver; he reports 73% overall reduction.

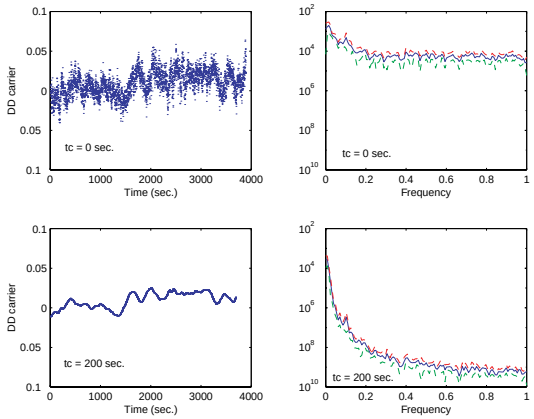

Figure 3. Effect of Time Averaging on Carrier Phase Measurement

If multipath and receiver error could be bounded by a normal distribution with standard deviation of 1% of a wavelength by using multipath mitigation techniques, along with time averaging, considerable improvement on integrity of the CIR can be achieved. Figur e4 shows probability of wrong integer rounding at each step in the CIR process over distance when the 1% value is used. Note that the probability of wrong EWL integer rounding is not shown on the plot as this value is lower than 10^{-9} even at the 20 km baseline.

The probability results in Figure 4 can be used to interpret integrity of the CIR over distance. For an application requiring integrity risk on the order of 10^{-8}, the EWL integer ambiguity is resolved since the probability of incorrect EWL integer resolution is less than 10^{-9} for all the tested distances. The WL integer ambiguity is resolved up to 6.9 km, where probability of incorrect WL integer ambiguity

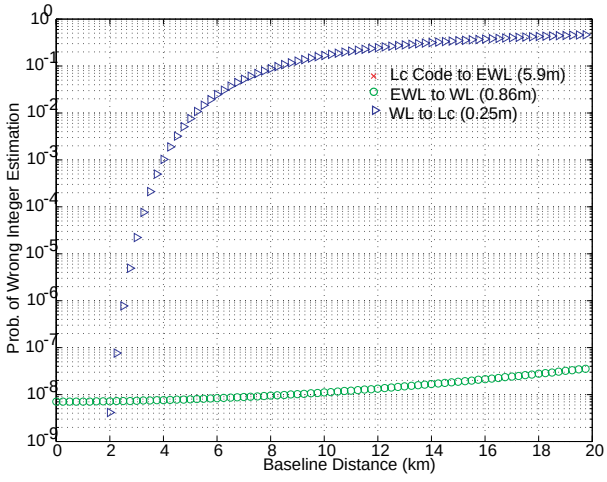

Figure 4. Integrity of the CIR Steps Over Distance. Carrier Phase Multipath and Receiver Error is 1% of Wavelength.

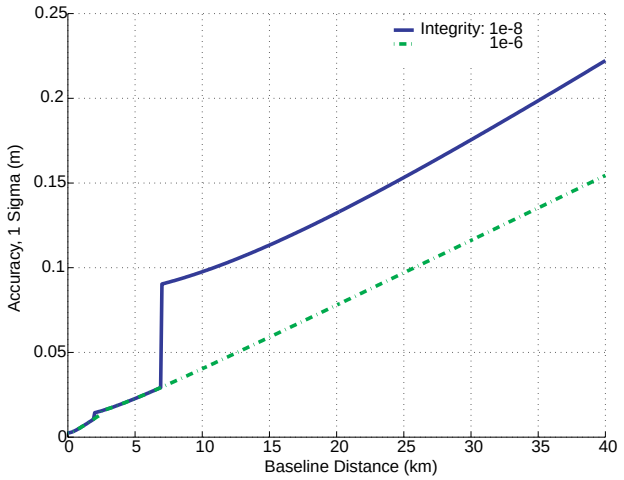

Figure 5. Level of Accuracy of the CIR Over Distance. Carrier Phase Multipath and Receiver Error is 1% of Wavelength.

resolution becomes higher than 10^{-8}. The Lc integer ambiguity is resolved up to 2.2 km, where probability of incorrect Lc integer ambiguity resolution becomes higher than 10^{-8}

For an application requiring integrity risk on the order of 10^{-6}, both the EWL and WL integer ambiguities are resolved since the probability of incorrect EWL and WL integer ambiguity resolution is less than 10^{-6} for all the tested distances. The Lc integer ambiguity is resolved up to 2.6 km, where probability of incorrect Lc integer ambiguity resolution becomes higher than 10^{-6}. Figure 5 shows the level of accuracy achieved by the CIR over distance for varying integrity requirements.

OPTIMIZATION OF THE CIR BY ESTIMATIING THE SPATIAL GRADIENT OF DIFFERENTIAL IONOSPHERE ERROR

Correction of Measurement Error due to Ionosphere

The pseudorange measurement error due to ionospheric effect varies from a few meters to tens of meters at the zenith, if uncorrected [4]. For a single frequency, stand alone user, a simple algorithm developed by Klobuchar [9] is used to correct for approximately 50% of the ionospheric range error. The algorithm corrects for the error by using the user's approximate geodetic latitude, longitude, elevation angle and azimuth to each GPS satellite, along with eight ionosphere coefficients included in the navigation message modulated on the C/A code.

By using DGPS, the range error due to ionosphere is reduced further. If the reference and user receivers are receiving a GPS satellite signal through the same ionospheric conditions, DGPS correction eliminates the range error due to ionosphere. However, the condition of the ionosphere decorrelates as the distance between the reference and user receivers increases. The spatial gradient of standard deviation of residual differential ionospheric error is assumed at 2 ppm in the analysis of the CIR, which uses double difference measurements. Figure 6 shows the increase in residual differential ionospheric error in the double difference measurement over growing baseline distance due to the spatial gradient.

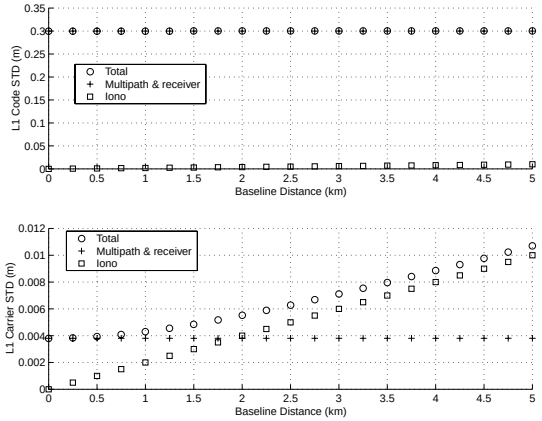

Figure 6. Effect of Residual Differential Ionosphere Error over Baseline Distance

For a user with a multiple frequency receiver, ionospheric range error is directly observed as it is a function of the carrier frequency of the GPS signal. For example, if the code and carrier phase measurements from the L1 and L2 frequencies are available, ionospheric range error is calculated by using the following equations.

$$\rho_{L1} - \rho_{L2} = (1 - \Upsilon_{12}) I_{L1} + \mu \tag{20}$$

$$\lambda_{L1}(\phi_{L1} - N_{L1}) - \lambda_{L2}(\phi_{L2} - N_{L2}) = (\Upsilon_{12} - 1) I_{L1} + \nu \tag{21}$$

Also, a linear combination of measurements from multiple frequencies can be formed in such a way as to eliminate the effect of ionosphere. The ionospheric-free linear combination of the L1 and L2 carrier phase measurement, shown in Equation (22), has a significant disadvantage, however. The integer ambiguity of the $\phi_{ionoFree}$ measurement is not an integer, since the integer ambiguity of the L2 carrier phase measurement is multiplied by f_{L2}/f_{L1}, which is a real number (0.7792), and the result is then subtracted from the L1 integer ambiguity.

$$\phi_{ionoFree} = \phi_{L1} - \frac{f_{L2}}{f_{L1}} \phi_{L2} \tag{22}$$

Improving Performance of the CIR by Estimating Spatial Gradient of Residual Differential Ionospheric Error

It was shown earlier that the probability of wrong integer estimation in the CIR is driven by measurement error. For a short baseline distance between the reference and user receivers, performance of the CIR is determined by double difference multipath and receiver error. However, as the baseline distance increases, probability of wrong integer estimation grows larger due to the increase in residual differential ionospheric error.

The spatial gradient of residual differential ionospheric error can be observed and treated as a state if measurements from two or more separate locations are used in the CIR. The measurement vector, **z**, the observation matrix, H, and the state vector, **u**, in Equation (7) are modified to carry out the covariance analysis with the spatial gradient as an additional state, by using measurements from two locations with a separation distance of Δb, as shown in Equation (23) and Figure 7.

$$z = Hu + \delta z \tag{23}$$

$$\begin{bmatrix} \rho_{1\alpha} \\ \rho_{2\alpha} \\ \rho_{c\alpha} \\ \phi_{1\alpha} \\ \phi_{2\alpha} \\ \phi_{c\alpha} \\ \rho_{1\beta} \\ \rho_{2\beta} \\ \rho_{c\beta} \\ \phi_{1\beta} \\ \phi_{2\beta} \\ \phi_{c\beta} \end{bmatrix} = \begin{bmatrix} 1 & 0 & b & 0\ 0\ 0 \\ 1 & 0 & \Upsilon_{12} b & 0\ 0\ 0 \\ 1 & 0 & \Upsilon_{1c} b & 0\ 0\ 0 \\ 1/\lambda_1 & 0 & -b/\lambda_1 & 1\ 0\ 0 \\ 1/\lambda_2 & 0 & -\Upsilon_{12} b/\lambda_2 & 0\ 1\ 0 \\ 1/\lambda_c & 0 & -\Upsilon_{1c} b/\lambda_c & 0\ 0\ 1 \\ 0 & 1 & (b+\Delta b) & 0\ 0\ 0 \\ 0 & 1 & \Upsilon_{12}(b+\Delta b) & 0\ 0\ 0 \\ 0 & 1 & \Upsilon_{1c}(b+\Delta b) & 0\ 0\ 0 \\ 0 & 1/\lambda_1 & -(b+\Delta b)/\lambda_1 & 1\ 0\ 0 \\ 0 & 1/\lambda_2 & -\Upsilon_{12}(b+\Delta b)/\lambda_2 & 0\ 1\ 0 \\ 0 & 1/\lambda_c & -\Upsilon_{1c}(b+\Delta b)/\lambda_c & 0\ 0\ 1 \end{bmatrix} \begin{bmatrix} R_\alpha \\ R_\beta \\ \nabla I_1 \\ N_1 \\ N_2 \\ N_c \end{bmatrix} + \begin{bmatrix} \delta\rho_{1\alpha} \\ \delta\rho_{2\alpha} \\ \delta\rho_{c\alpha} \\ \delta\phi_{1\alpha} \\ \delta\phi_{2\alpha} \\ \delta\phi_{c\alpha} \\ \delta\rho_{1\beta} \\ \delta\rho_{2\beta} \\ \delta\rho_{c\beta} \\ \delta\phi_{1\beta} \\ \delta\phi_{2\beta} \\ \delta\phi_{c\beta} \end{bmatrix}$$

With the updated observation matrix and measurement error vector, the covariance analysis of the state estimation developed earlier is used to calculate the probability of incorrect integer resolution of each step in the CIR. Figure 8 shows improvements in the probability of wrong WL and Lc integer estimation when the spatial gradient of

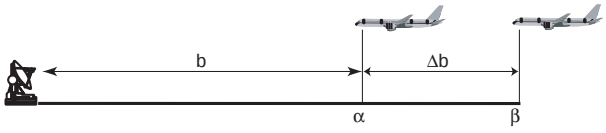

Figure 7. Estimating the Spatial Gradient of Residual Differential Ionospheric Error

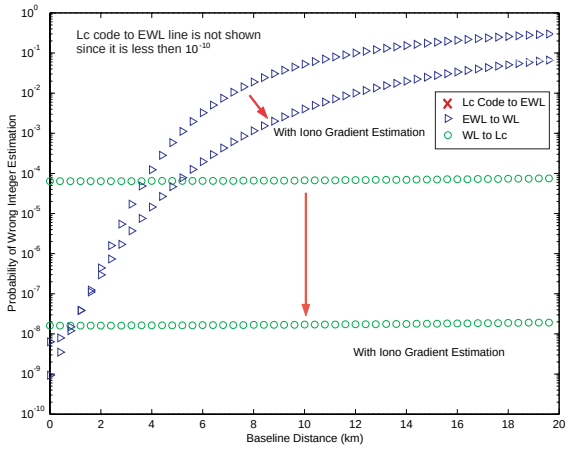

Figure 8. Probability of Wrong Integer Estimation, Δb =10 km

residual differential ionospheric error is estimated by using measurements from two locations separated by 10 km. The probability of wrong EWL integer estimation by using the Lc code measurements in both cases is lower than 10^{-10} and hence is not shown on the plot.

When the spatial gradient is estimated with Δb = 10 km, the CIR can be used to resolve the Lc integer ambiguity up to 4 km, instead of up to 2.4 km without the estimation, with probability of incorrect integer resolution of 10^{-4}. It can also resolve the WL integer ambiguity up to 40 km with the estimation, instead of up to 22 km without the estimation, with the same probability. Clearly, by estimating the spatial gradient, performance of the CIR is improved. In Figure 9, a comparison of performance of the CIR over distance for a desired level of integrity with (circle in Figure 9) and without estimation (triangle in Figure 9) of

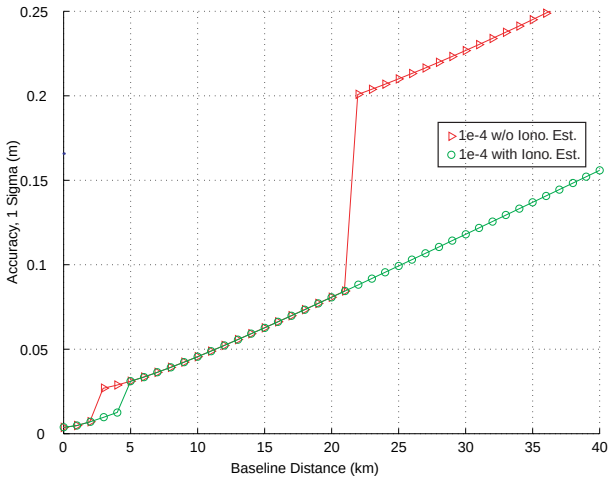

Figure 9. Improved Performance of the CIR with Estimation of the Spatial Gradient

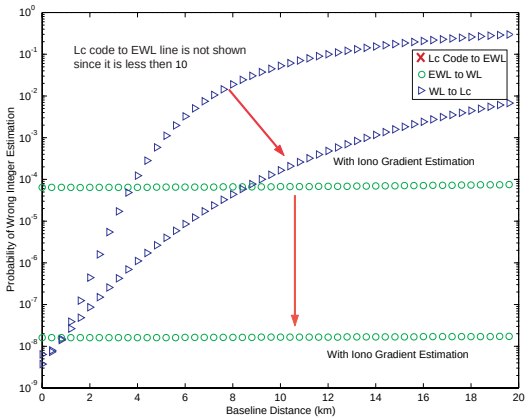

Figure 10. Probability of Wrong Integer Estimation, Δb =20 km

the spatial gradient of residual differential ionospheric error is shown

In Figure 10, it is shown that the larger the separation distance between the measurements, Δb km, the greater the improvement due to increased observability on the spatial gradient. However, since the estimated states now include the effect of change in geometry of the satellite as the user moves from one location to the other for multiple measurements, the CIR with spatial gradient of residual differential ionospheric error estimation is no longer a geometry-free process. Although the effect of change in satellite geometry should further improve performance of the CIR, it is not analyzed in this paper. Also, the user receiver is assumed to maintain the lock on the GPS carrier as the user moves between the measurement points. If the lock is reset, additional integer ambiguity resolution is required for each carrier phase measurement at the new measurement location.

COLCLUSION

A very accurate pseudorange can be acquired by using carrier phase measurement of the GPS signal, if its integer ambiguity is resolved. The Cascade Integer Resolution uses the longer wavelength of beat frequencies of multiple GPS carrier frequencies as “stepping stones” to resolve the integer ambiguity.

Due to its cascading nature, integrity of the integer estimation of each step must meet a desired level before the CIR process progresses. The integrity of each integer resolution step is investigated by using covariance analysis with five states: pseudorange, ionosphere delay, integer ambiguity for the L1, L2 and Lc, and with six measurements: three C/A code and three carrier phase measurements. Covariance analysis is used to calculate the probability of estimating the right EWL, WL and ML integers. Results from these integrity analyses are used to find the service distance or coverage area of the CIR, with a given desired probability of incorrect integer resolution. For an application requiring integrity risk on the order of 10^{-4}, the CIR can be used to resolve the Lc integer ambiguity up to 2.4 km, the WL integer ambiguity up to 22 km, and the EWL integer ambiguity beyond 22 km. Table 4 summarizes the performance of the CIR.

Table 4. Resolved Integer Ambiguity by the CIR for Different Levels of Integrity, k=2% of Wavelength

	Resolved Integer Ambiguity		
Desired Integrity	Lc	WL	EWL
10^{-8}	cannot resolve	cannot resolve	up to 40+km
10^{-6}	cannot resolve	cannot resolve	up to 40+km
10^{-4}	up to 2.4 km	up to 22 km	up to 40+km

If the standard deviation of double differenced multipath and receiver error could be reduced to 1% of a wavelength by using multipath mitigation techniques, along with time averaging, considerable improvement on integrity of the CIR can be achieved. Table 5 summarizes the improvement of the CIR performance due to decrease in measurement error.

Table 5. Resolved Integer Ambiguity by the CIR for Different Levels of Integrity, with Reduced Measurement Error (k=1%)

	Resolved Integer Ambiguity		
Desired Integrity	Lc	WL	EWL
10^{-8}	up to 2 km	up to 6.7 km	up to 40+km
10^{-6}	up to 2.6 km	up to 40 +km	up to 40+km
10^{-4}	up to 2.6 km	up to 40+ km	up to 40+km

The spatial gradient of standard deviation of residual differential ionospheric error was first assumed to be 2 ppm. It is used as *a priori* information in the covariance analysis. However, the spatial gradient is observable if measurements from two or more separate locations are used in the CIR. When measurements from locations 10 km apart are used to estimate the spatial gradient, the performance of the CIR improved. For a desired probability of incorrect integer ambiguity resolution of 10^{-4}, the Lc integer is resolved up to 4 km instead of up to 2.4 km without estimation of the spatial gradient. Also, the WL integer is resolved up to 40 km with the estimation, instead of 22 km without, for the

same probability. However, the CIR process is no longer geometry free when the multiple measurements are used to estimate the spatial gradient of differential ionospheric error.

The Cascade Integer Resolution is developed to utilize multiple civil GPS signals to guide users to their destinations accurately and reliably. By instantaneously estimating the integer ambiguity with relatively low probability of incorrect resolution, the CIR is well suited for use in CDGPS with the three civil GPS signals available in the near future.

BIBLIOGRAPHY

[1] Axelrad, Penina, Christopher Comp and Peter MacDoran. Use of Signal -To-Noise Ratio for Multipath Error Correction in GPS Differential Phase Measurements: Methodology and Experimental Results. Proc. of ION GPS. Vol. 1, 1994, Salt Lake, Utah, Alexandria: The Institute of Navigation, 1994.

[2] Braasch, Michael S. GPS Multipath Model Validation. Proc. of IEEE Position Location and Navigation Symposium, 1996, New York, NY. New York: The Institute of Electrical and Electronics Engineering, Inc. 1996.

[3] Braasch, Michael S. Isolation of GPS Multipath and Receiver Tracking Errors. Navigation. Vol. 41, No. 4, Winter 1994-1995. Alexandria: The Institute of Navigation, 1995.

[4] Christie, Jock R. I., Ping-Ya Ko, Andrew Hansen, Donghai Dai, Samuel Pullen, Boris S. Pervan, and Bradford W. Parkinson. The Effect of Local Ionospheric Decorrelation on LAAS: Theory and Experimental Results. Proc. of ION NTM. January 1999, San Diego, California, Alexandria: The Institute of Navigation, 1999.

[5] Forssell, B., M. Martin-Neira, and R. A. Harris. Carrier Phase Ambiguity Resolution in GNSS-2. Proc. of ION GPS. Vol. 2, 1997, Kansas City, Missouri. Alexandria: The Institute of Navigation, 1997.

[6] Gomez, Susan, Robert Panneton, and Penny Saunders. GPS Multipath Modeling and Verification Using Geometrical Theory of Diffraction. Proc. of ION GPS. Vol. 1, 1995, Palm Springs, California. Alexandria: The Institute of Navigation, 1995.

[7] Han, Shaowei. Carrier Phase-Based Long-Range GPS Kinematic Positioning. UNISURV Report S-49, 1997. New South Wales: University of New South Wales, 1997.

[8] Jung, Jaewoo. High Integrity Carrier Phase Navigation for Future LAAS Using Multiple Civilian GPS Signals. Proc. of ION GPS. 1999, Nashville, Tennessee. Alexandria: The Institute of Navigation, 1999.

[9] Klobuchar, J. A. “Ionospheric Effects on GPS.” Global Positioning System: Theory and Applications. Ed. Bradford W. Parkinson et al. Vol. 1. Washington DC: American Institute of Aeronautics and Astronautics, Inc. 1996.

[10] Ray, Jayanta Kumar. Mitigation of Static Carrier Phase Multipath Effects Using Multiple Closely-Spaced Antennas. Proc. of ION GPS.Vol. 2, 1998, Nashville, Tennessee. Alexandria: The Institute of Navigation, 1998.

[11] Vollath, Ulrich, S. Birnbach, H. Landau, J. M. fraile-Ordonez, and M. martin-Neira. Analysis of Three-Carrier Ambiguity Resolution (TCAR) technique for Precise Relative Positioning in GNSS-2. Proc. of ION GPS 1998. Vol. 1. Alexandria: The Institute of Navigation, 1998.

[12] Werner, Wolfgang, Bernd Eissfeller, Zonghou Fu and Gunter W. Hein. Performance of the TCAR Method in Multipath and Jamming Environments. Proc. of ION GPS 1998. Alexandria: The Institute of Navigation, 1998.

[13] Wu. J. and S. G. Lin. Height Accuracy of One and a Half Centimeters by GPS Rapid Static Surveying. International Journal of Remote Sensing. Vol. 16. No. 15. October 1995.

[14] Wu. J. and S. G. Lin. Kinematic Positioning with GPS Carrier Phases by Two Types of Wide Laning. Navigation. Vol. 44. No. 4. Winter 1997-1998. Alexandria: The Institute of Navigation, 1998.